Physica A 525 (2019) 566–575

Contents lists available at ScienceDirect

Physica A

journal homepage: www.elsevier.com/locate/physa

The effect of Headway Variation Tendency on traffic flow: Modeling and stabilization

Tao Wang [a,*], Guangyao Li [a], Jing Zhang [b], Shubin Li [c], Tao Sun [d]

[a] Department of Automation and Electronic Engineering, Qingdao University of Science and Technology, Qingdao, 266061, China
[b] School of Mathematics and Physics, Qingdao University of Science and Technology, Qingdao 266061, China
[c] Department of Traffic Management Engineering, Shandong Police College, Jinan, 250014, China
[d] Traffic Management Bureau, Public Security Department of Shandong Province, Jinan 250031, China

HIGHLIGHTS

- An improved car-following model is proposed by considering the effect of Headway Variation Tendency (HVT).
- The linear stability condition and the modified KdV equation are derived.
- The numerical simulation is presented to verify the effect of the headway variation tendency on traffic flow.
- Both the analytical and simulation results show that HVT can attenuate disturbance and avoid serious traffic jam effectively.

ARTICLE INFO

Article history:
Received 6 December 2018
Received in revised form 2 March 2019
Available online 2 April 2019

Keywords:
Car-following model
Headway Variation Tendency
Traffic flow
mKdV equation

ABSTRACT

Advanced communications technology enables us to obtain the Headway Variation Tendency (HVT) of the next moment in a car following scenario. To maximize the benefits of the new technology, we developed a new traffic flow model that takes into consideration the effect of HVT. First, linear analysis method is used to derive the linear stability condition, that determines whether the HVT can improve traffic system stability. Then, using the reductive perturbation method, a modified KdV (mKdV) equation is obtained and the kink–antikink solutions are derived. The phase diagram of driver sensitivity against equilibrium headway is also plotted by using the neutral stability line, derived from linear analysis and the coexisting line, derived from nonlinear analysis. This diagram demonstrates that HVT does have the ability to improve the stability of traffic stream. Finally, the effect of HVT is validated through numerical simulations, where it is evident that the information of HVT can smooth the traffic stream and prevent the formation of traffic congestion.

1. Introduction

The growing traffic jam causes excessive fuel consumption as well as emissions to the urban environment. Such adverse impacts pose a severe threat to the traffic system performance. Various traffic flow models have been developed, to explore the mechanism of traffic jam formation [1–40]. Generally, traffic flow models are divided into macroscopic models based on fluid mechanics, mesoscopic models based on gas dynamics theory and microscopic models based on self-driven particles. The macroscopic models include continuum [1–5] and lattice hydrodynamic models [6–13]. The mesoscopic

* Corresponding author.
E-mail address: twang@qust.edu.cn (T. Wang).

https://doi.org/10.1016/j.physa.2019.03.116
0378-4371/

models [14], as a bridge between microscopic and macroscopic models, can capture the probabilistic nature of interactions between vehicles and describe the macroscopic characteristics of the traffic system. The microscopic models investigate the movement of the individual vehicle, and mainly include cellular automata [15–19], car-following models [20–28] and application of microscopic models in various scenarios [29–34].

With the advent of Connected Vehicle Technology (CVT), drivers can access accurate shared information about other vehicles, such as vehicle position, velocity, space headway and even acceleration. By considering the effect of multiple headway, Ge et al. [35] proposed a cooperative driving model, where the theoretical analysis and the numerical simulation both demonstrate that, introducing more than one site ahead in vehicle motion, can improve the traffic system stability. Jiang et al. found that the negative speed difference can also influence driving behavior in a general force model [36], so they proposed a new traffic flow model [37] which is able to describe the effect of positive velocity difference. Considering the effect of multi-vehicle speed differences, Wang et al. [38] constructed a cooperative traffic flow model to study the impact of multiple velocity differences on traffic flow dynamics. Besides considering the influence of the position and velocity on the traffic system, some researchers take the acceleration [39] and even the jerk (i.e., rate of change of acceleration) [40] into account, in order to improve traffic system stability.

Recently, the research on the anticipation effect has attracted great attention since it is a universal psychological phenomenon in drivers. Tang et al. [41,42] examined how the driver's forecast effect (DFE) influences traffic system stability. Based on the microscopic analysis, they further researched the macro influences of DFE on traffic system. The anticipation effect on dynamics of traffic flow is also analyzed using the lattice hydrodynamic model [43]. By considering the effect of anticipation on traffic flow, Zheng et al. [44] examined the anticipation effect within a microscopic traffic model. As a key parameter of traffic flow stability, anticipation optimal velocity is introduced into both microscopic and macroscopic models [45,46]. Although various values of the anticipation effect are introduced to the traffic flow model stabilizing the traffic stream, the effect of the expect Headway Variation Tendency (HVT), i.e. the headway variation resulting from the driver behavior of the direct leading vehicle, is not explored.

The information of HVT can lead drivers following the leading car smoothly under congestion situation. For example, if a driver can prejudge his/her future headway variation tendency, according to the driving behavior of the leading vehicle, he/she will accelerate (decelerate) in advance. Such operation can compensate the human driver's delay which is one main contribution to traffic jam. Therefore, the HVT can reduce the generation of small disturbances and thus prevent the formation of traffic congestion. The contribution of this paper focuses on: (1) construction of a new traffic flow model considering the impact of HVT; (2) implementation of analytical method to deduce the theoretical results describing the impact of HVT on traffic stability; (3) analysis of different model parameters' impact on traffic system, using numerical method.

The structure of this paper is as follows: the improved model is introduced in Section 2. The linear stability condition of the proposed model is described in Section 3. The mKdV equation is derived by a nonlinear method in Section 4. In Section 5, the analytical results are tested in numerical simulations. Conclusions are described in Section 6.

2. The new model

Traffic flow models have been tested since 1950 [20]. Among them, the Newell model is widely applied for its simplicity, intuitiveness and innovativeness [21]. The trajectory of nth car is described by a set of coupled differential equations:

$$\frac{dx_n(t+\tau)}{dt} = V\left(\Delta x_n(t)\right) \tag{1}$$

Where $x_n(t+\tau)$, is the position of vehicle n at time $t+\tau$, $\Delta x_n(t) = x_{n+1}(t) - x_n(t)$ is the headway, τ is the time space where drivers adjust their speed. According to the Newell model, drivers adjust their speed in line with space headway within adjusting time τ.

In a normal traffic system, every car is moving. The current car can run faster or slower to avoid accelerating or decelerating frequently if we know the leading car's movement behavior of next moment. This action will prevent the small disturbance occurring and smooth traffic system, and therefore stabilize traffic flow. Based on the Newell approach, we propose a new car-following model that additionally takes into account the impact of HVT, described mathematically as follows:

$$\frac{dx_n(t+\tau)}{dt} = V\left(\Delta x_n(t) + \lambda\left(\Delta x_n(t+\tau_1) - \Delta x_n(t)\right)\right) \tag{2}$$

Where, τ_1 is anticipative time, λ is effect coefficient of HVT ($0 \le \lambda < 1$), $\lambda\left(\Delta x_n(t+\tau_1) - \Delta x_n(t)\right)$ is the impact of HVT. In our proposed model, the speed of vehicles depends not only on the space headway $\Delta x_n(t)$, but also on the HVT. Therefore, the new model can be used to explore the impact of HVT on traffic flow dynamics.

For simplicity, using Taylor's expansion, it can be said that:

$$\begin{aligned} &V\left(\Delta x_n(t) + \lambda\left(\Delta x_n(t+\tau_1) - \Delta x_n(t)\right)\right) \\ &\approx V\left(\Delta x_n(t)\right) + \lambda\left(\Delta x_n(t+\tau_1) - \Delta x_n(t)\right) V'\left(\Delta x_n(t)\right). \end{aligned} \tag{3}$$

We rewrite the new model as:

$$\frac{dx_n(t+\tau)}{dt} = V\left(\Delta x_n(t)\right) + \lambda\left(\Delta x_n(t+\tau_1) - \Delta x_n(t)\right) V'\left(\Delta x_n(t)\right) \tag{4}$$

By converting the time derivative to an asymmetric forward difference, Eq. (4) can be rewritten as a difference equation:

$$x_n(t+2\tau) = x_n(t+\tau) + \tau V\left(\Delta x_n(t)\right) + \lambda\tau\left(\Delta x_n(t+\tau_1) - \Delta x_n(t)\right) V'(\Delta x_n(t)) \tag{5}$$

In this work, we adopt the widely accepted optimal velocity definition, as described by Bando et al. [22],

$$V\left(\Delta x_n(t)\right) = \frac{v_{\max}}{2}\left(\tanh\left(\Delta x_n(t) - h_c\right) + \tanh(h_c)\right) \tag{6}$$

Using asymmetric difference method to discretize the proposed model, the simplified version of Eq. (4) reads:

$$\begin{aligned}\Delta x_n(t+2\tau) &= \Delta x_n(t+\tau) + \tau\left(V\left(\Delta x_{n+1}(t)\right) - V\left(\Delta x_n(t)\right)\right)\\ &+ \lambda\tau[V'\left(\Delta x_{n+1}(t)\right)\left(\Delta x_{n+1}(t+\tau_1) - \Delta x_{n+1}(t)\right)\\ &- V'\left(\Delta x_n(t)\right)\left(\Delta x_n(t+\tau_1) - \Delta x_n(t)\right)]\end{aligned} \tag{7}$$

3. Linear stability analysis

In view of the stability of uniformly steady-state flow, the extended model in Eq. (4) is processed using the linear stability method. It is obvious that the steady state can be defined by assuming the vehicles running at the same optimal speed $V(h)$ and maintaining a uniform headway space h. Therefore, the uniform steady-state solution of Eq. (4) can be described by

$$x_{n,0}(t) = hn + V(h)t,\ h = L/N \tag{8}$$

Where N denotes the total number of cars, L is the road length.

Assuming $y_n(t)$ is a slight deviation from the steady-state solution:

$$x_n(t) = x_{n,0}(t) + y_n(t) \tag{9}$$

Using $V'(\Delta x_n) = V'(h + \Delta y_n) \approx V'(h) + V''(h)\Delta y_n$, and substituting Eq. (9) into Eq. (7), we get

$$\begin{aligned}&\Delta y_n(t+2\tau)\\ &= \Delta y_n(t+\tau) + \tau V'(h)\left(\Delta y_{n+1}(t) - \Delta y_n(t)\right)\\ &+ \lambda\tau V'(h)\left(\Delta y_{n+1}(t+\tau_1) - \Delta y_n(t+\tau_1) - \Delta y_{n+1}(t) + \Delta y_n(t)\right)\end{aligned} \tag{10}$$

Where $V'(h) = \left.\frac{dV(\Delta x_n)}{d\Delta x_n}\right|_{\Delta x=h}$ and $\Delta y_n(t) = y_{n+1}(t) - y_n(t)$.

Through expanding $\Delta y_n(t) = Ae^{ink+zt}$, one obtains:

$$e^{2z\tau} - e^{z\tau} - \tau V'(h)(e^{ik} - 1) - \lambda\tau V'(h)(e^{ik+z\tau_1} - e^{z\tau_1} - e^{ik} + 1) = 0 \tag{11}$$

Letting $z = z_1 ik + z_2(ik)^2 + \cdots$ and substituting the expansions of z into Eq. (11), ignoring the terms of order greater than two, lead to the following two roots of z:

$$z_1 = V'(h)$$

$$z_2 = \frac{1}{2}V'(h) - \frac{3}{2}V'^2(h)\tau + \lambda\tau_1 V'^2(h) \tag{12}$$

When $z_2 < 0$, for slight perturbation with long wavelengths, the flow will tend to be unstable. When $z_2 > 0$, the uniformly steady-state flow is stable. Thus, the neutral stability condition can be as follows:

$$\tau = \frac{1 + 2\lambda\tau_1 V'(h)}{3V'(h)} \tag{13}$$

If the following condition is met, the unstable traffic flow will be generated due to the slight disturbances in the uniform flow.

$$\tau > \frac{1 + 2\lambda\tau_1 V'(h)}{3V'(h)} \tag{14}$$

Eq. (13) shows that the neutral curve is moving lower as the impact intensity of HVT increases, so by considering the impact of HVT the traffic flow can be stabilized.

4. Nonlinear stability analysis

In order to investigate the impact of HVT on traffic stream stability, we adopt the method of nonlinear analysis on Eq. (7) and on the slowly varying behavior around critical points. Here, $0 < \varepsilon \ll 1$. So, the slow variables X and T are defined as:

$$X = \varepsilon(n + bt), T = \varepsilon^3 t \tag{15}$$

Where, b is a constant. Let

$$\Delta x_n(t) = h_c + \varepsilon R(X, T) \tag{16}$$

We first substitute Eqs. (15) and (16) into Eq. (7), then consider the Taylor expansions to the 5th order of ε, thereby getting the following equation:

$$\begin{aligned}
&\varepsilon^2(b - V')\partial_X R + \varepsilon^3(\frac{3}{2}b^2\tau - \frac{1}{2}V' - V'\lambda\tau_1 b)\partial_X^2 R \\
&+ \varepsilon^4(\frac{7}{6}b^3\tau^2\partial_X^3 R - \frac{1}{6}V'''\partial_X R^3 - \frac{1}{6}V'\partial_X^3 R - \lambda V'\frac{b^2\tau_1^2 + b\tau_1}{2}\partial_X^3 R + \partial_T R) \\
&+ \varepsilon^5(\frac{5}{8}b^4\tau^3\partial_X^4 R + 3b\tau\partial_T\partial_X R - \frac{1}{12}V'''\partial_X^2 R^3 - \frac{1}{24}V'\partial_X^4 R \\
&- \lambda V'\frac{2b^3\tau_1^3 + 3b^2\tau_1^2 + 2b\tau_1}{12}\partial_X^4 R - \lambda\tau_1 V'\partial_T\partial_X R) = 0
\end{aligned} \tag{17}$$

Where

$$V'(h_c) = \left.\frac{dV(\Delta x_n)}{d\Delta x_n}\right|\Delta x_n = h_c \quad \text{and} V'''(h_c) = \left.\frac{d^3V(\Delta x_n)}{d\Delta x_n^3}\right|\Delta x_n = h_c$$

Let $b = V'$ and around the critical point τ_c, we have

$$\frac{\tau}{\tau_c} = 1 + \varepsilon^2 \tag{18}$$

To simplify Eq. (17), we omit the 2nd and 3rd order terms of ε, so Eq. (17) can be rewritten as:

$$\varepsilon^4(\partial_T R - g_1\partial_X^3 R + g_2\partial_X R^3) + \varepsilon^5(g_3\partial_X^2 R + g_4\partial_X^4 R + g_5\partial_X^2 R^3) = 0 \tag{19}$$

where

$$\begin{aligned}
g_1 &= -\frac{V'}{6}[\frac{7}{9}(1 + 2\tau_1\lambda V')^2 - 1 - 3\tau_1\lambda V'(V'\tau_1 + 1)] \\
g_2 &= -\frac{V'''}{6} \\
g_3 &= \frac{V' + 2\tau_1\lambda V'^2}{2} \\
g_4 &= \frac{5(1 + 2\lambda\tau_1 V')}{216} - \frac{V'}{24} - \lambda V'\frac{2(\tau_1 V')^3 + 3(\tau_1 V')^2 + 2V'\tau_1}{12} \\
&\quad -(1 + \lambda\tau_1 V')[\tfrac{V'}{6}(\tfrac{7}{9}(1 + 2\lambda\tau_1 V')^2 - 1 - 3\lambda\tau_1 V'(V'\tau_1 + 1))] \\
g_5 &= \frac{2(1 + \lambda\tau_1 V')V''' - V'''}{12}
\end{aligned} \tag{20}$$

To obtain the regularized equation, the conversion can be performed on the Eq. (19) as follows:

$$\begin{aligned}
T' &= -\frac{V'}{6}\left[\frac{7}{9}(1 + 2\tau_1\lambda V')^2 - 1 - 3\tau_1\lambda V'(\tau_1 V' + 1)\right]T \\
R &= \sqrt{\frac{V'\left[\frac{7}{9}(1 + 2\lambda\tau_1 V')^2 - 1 - 3\lambda\tau_1 V'(\tau_1 V' + 1)\right]}{V'''}}R'
\end{aligned} \tag{21}$$

The standard mKdV equation with a $O(\varepsilon)$ correction term is as follows:

$$\partial_{T'}R' - \partial_X^3 R' + \partial_X R'^3 + \varepsilon\sqrt{\frac{1}{g_1}}(g_3\partial_X^2 R' + \frac{g_1 g_5}{g_2}\partial_X^2 R'^3 + g_4\partial_X^4 R') = 0 \tag{22}$$

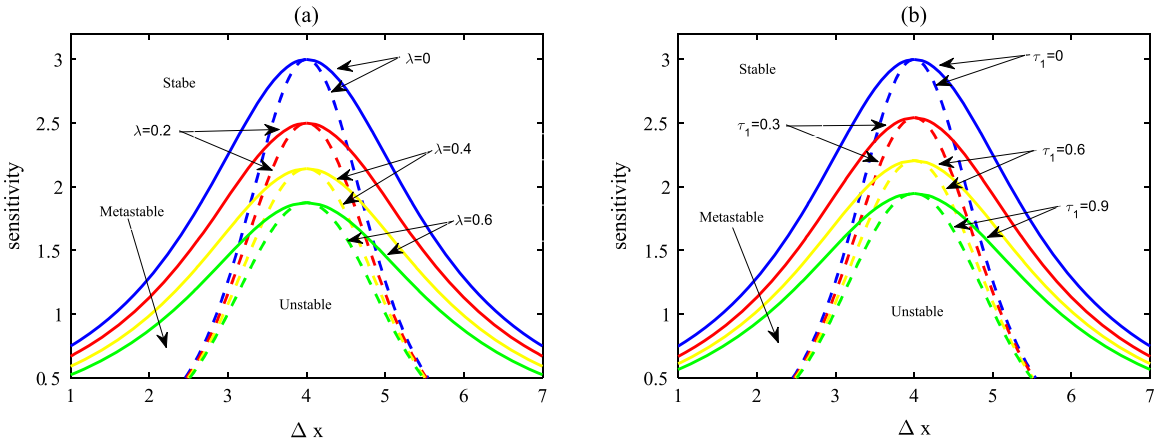

Fig. 1. Phase diagram in headway-sensitivity space $(\Delta x, \alpha)$.

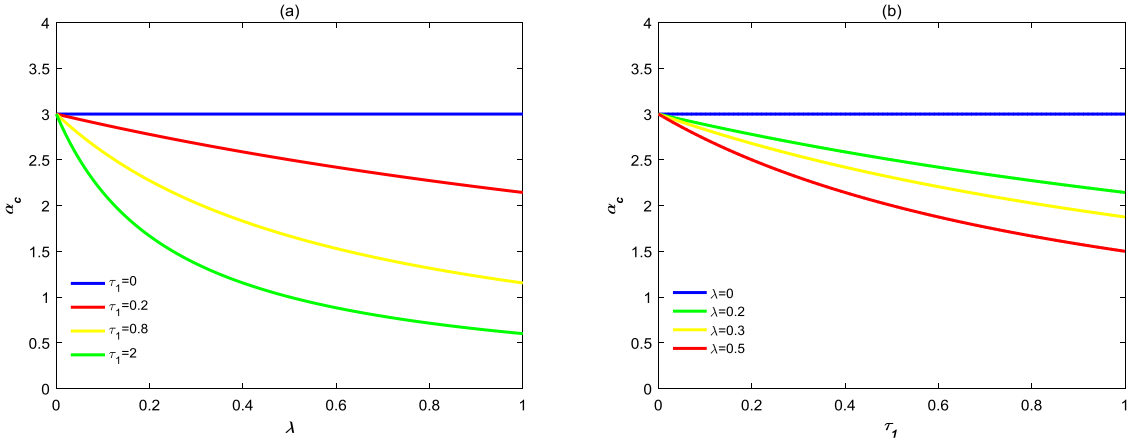

Fig. 2. The relation diagram between the sensitivity α_c and the effect coefficient of HVT λ and the relation diagram between the sensitivity α_c and the anticipation time τ_1.

If the perturbed term $O(\varepsilon)$ is omitted, the mKdV equation with the kink–antikink soliton solution is:

$$R_0'(X, T') = \sqrt{c}\tanh\left(\sqrt{\frac{c}{2}}(X - cT')\right) \tag{23}$$

where c is the propagation velocity of the density wave. The selected value of velocity can be obtained if Eq. (24) is satisfied,

$$(R_0', M[R_0']) \equiv \int_{-\infty}^{+\infty} dX R_0'(X, T') M[R_0'(X, T')] = 0 \tag{24}$$

where

$$M[R'] = \sqrt{\frac{1}{g_1}}(g_3\partial_X^2 R' + \frac{g_1 g_5}{g_2}\partial_X^2 R'^3 + g_4\partial_X^4 R') \tag{25}$$

The selected speed c can be obtained by performing integration

$$c = \frac{5g_2g_3}{2g_2g_4 - 3g_1g_5} \tag{26}$$

Then, the solution of kink–antikink soliton can be derived as

$$(V' = V_{\max}/2 = 1, V''' = -V_{\max} = -2),$$

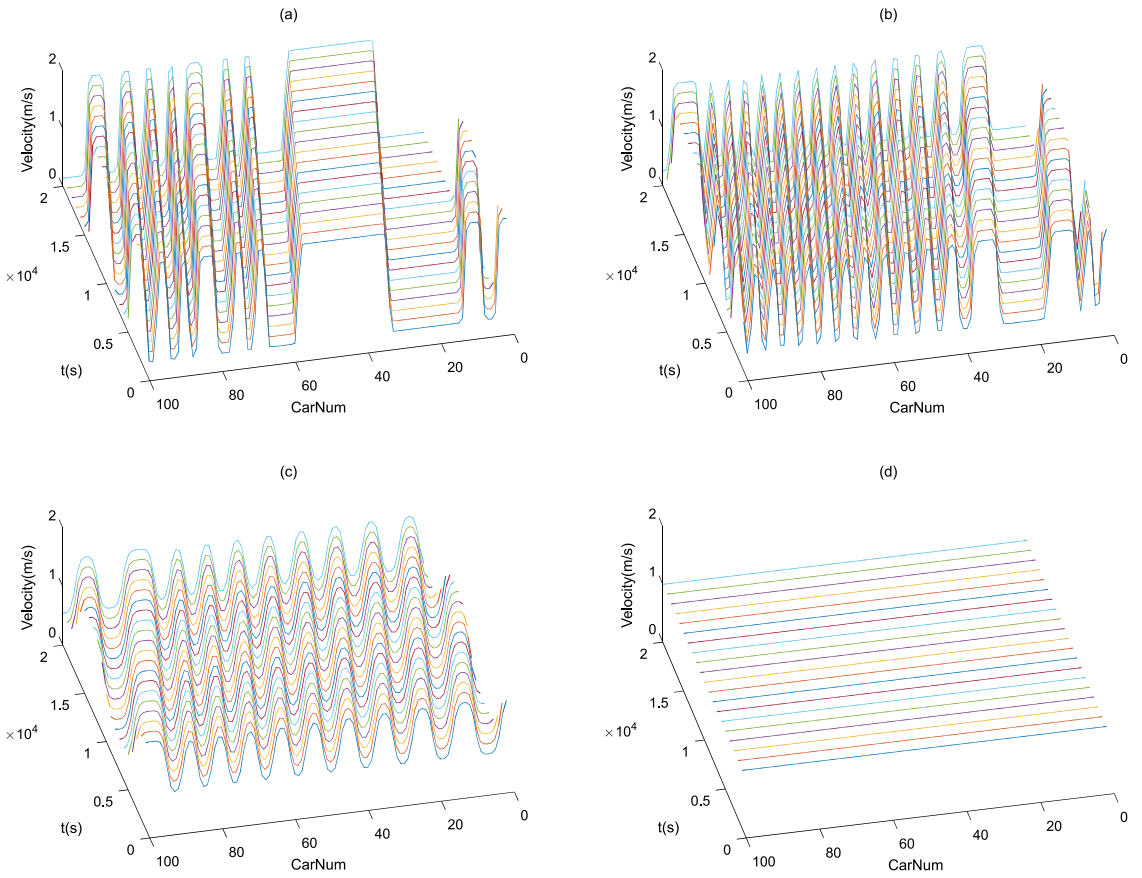

Fig. 3. The velocity evolution after $t = 10\,000$ s under the different parameters λ: (a) $\lambda = 0$, $\tau_1 = 0.5$, (b) $\lambda = 0.2$, $\tau_1 = 0.5$, (c) $\lambda = 0.4$, $\tau_1 = 0.5$, (d) $\lambda = 0.6$, $\tau_1 = 0.5$.

$$R(X,T) = \sqrt{\frac{g_1}{g_2}}\tanh\sqrt{\frac{c}{2}}(X - g_1 cT) \tag{27}$$

The amplitude A of the solution is

$$A = \sqrt{\frac{g_1 c}{g_2}\left(\frac{\alpha_c}{\alpha} - 1\right)} \quad with \quad \alpha_c = \frac{1}{\tau_c} = \frac{3V'}{1 + 2\lambda\tau_1 V'} \tag{28}$$

The kink–antikink wave solution represents a coexistence phase including low-density free-flow phase and high-density jammed phase. The relating space headways are presented by $\Delta x = h_c + A$ and $\Delta x = h_c - A$, respectively.

We plotted the coexisting and the neutral stability curves in Fig. 1, where the coexisting curve is indicated by solid line and the neutral curve is indicated by dotted line. Fig. 1(a) shows phase diagram of the space headway-sensitivity under different values of λ and $\tau_1 = 0.5$, and Fig. 1(b) shows phase diagram of the space headway-sensitivity under different values of τ_1 and $\lambda = 0.3$. Fig. 1 demonstrates how each couple of parameters (λ, τ_1) have two curves, that divide the traffic system into three regions: the unstable region, the stable region and the meta-stable region. In the unstable region, disturbance of any size will be amplified and finally evolve into a congestion state. In the stable region, slight disturbance in the traffic system will not lead to traffic congestions, while in the metastable region, the pattern of traffic is determined by the size of perturbation. Fig. 1, shows that the unstable range decreases when λ or τ_1 increase, indicating that λ and τ_1 can strengthen the traffic stability.

To better understand the effects of λ and τ_1 on the traffic stability, we plotted the influence of parameters λ and τ_1 on critical sensitivity α_c (see Fig. 2). We can see that critical α_c is falling over λ or τ_1, which is consistent with Eqs. (14) and (28). The longer the anticipation time τ_1 or higher the effect coefficient λ is, the lower the critical sensitivity is, which indicates that the effect coefficient and the anticipation time can both stabilize traffic flow.

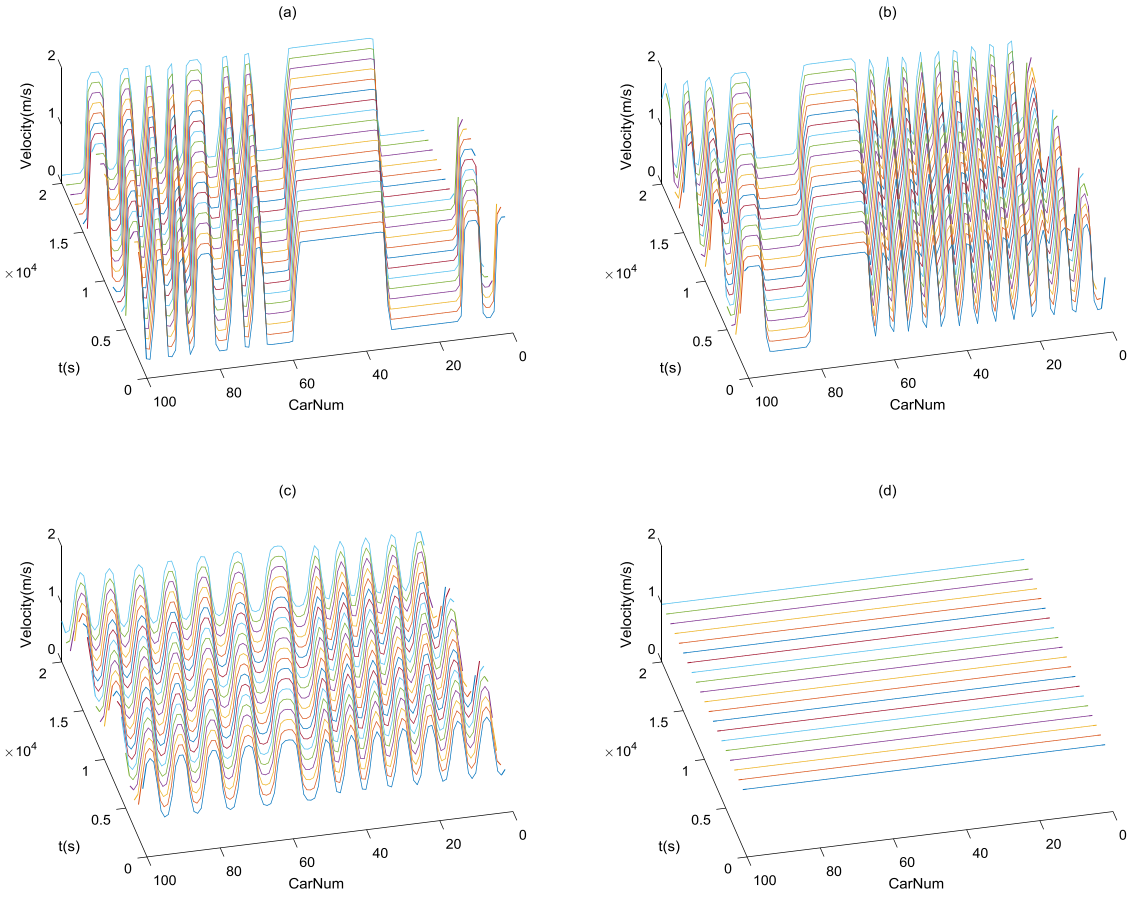

Fig. 4. Space–time evolution of velocity after $t = 10\,000$ s under the different parameters τ_1: (a) $\lambda = 0.3, \tau_1 = 0$, (b) $\lambda = 0.3, \tau_1 = 0.3$, (c) $\lambda = 0.3, \tau_1 = 0.6$, (d) $\lambda = 0.3, \tau_1 = 0.9$.

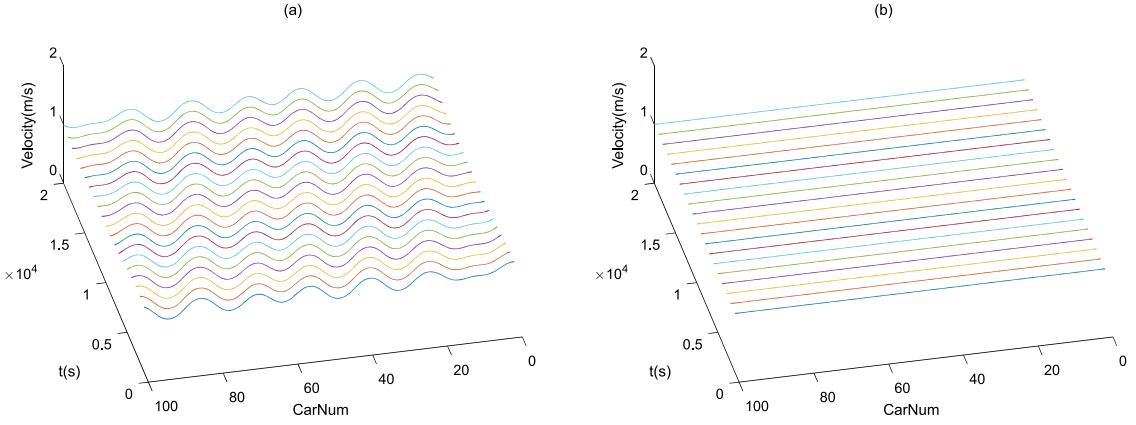

Fig. 5. Space–time evolution of velocity after $t = 10\,000$ s under the different parameters λ, τ_1: (a) $\lambda = 0.4, \tau_1 = 0.6$, (b) $\lambda = 0.5, \tau_1 = 0.7$.

5. Simulations

In order to study how traffic stability is affected by anticipation time and the effect coefficient of HVT, we carry out numerical simulations under a periodic boundary condition. In this paper, Eq. (7) is used to study the spatial-time evolution of the velocity with a small perturbation. Assuming $N = 100$ cars are running on a circuit road with $L = 400$ m. Let the initial conditions be as: $\Delta x_n(0) = 4.0$, $\Delta x_n(1) = 4.0$ for $n \neq 50, 51$, $\Delta x_n(0) = 4.0 - 0.1$, $\Delta x_n(1) = 4.0 - 0.1$

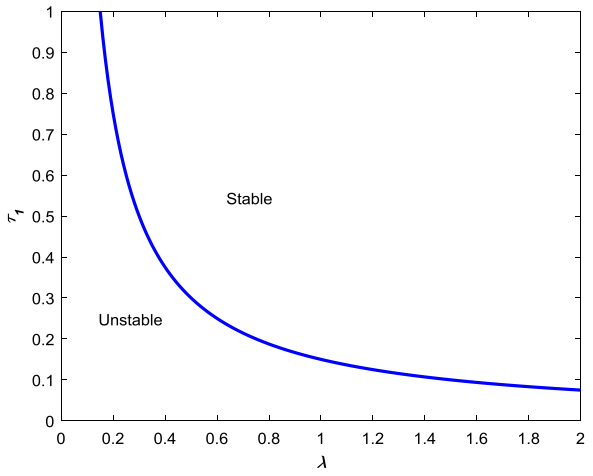

Fig. 6. Phase diagram in the space (λ, τ_1).

for $n = 50$, and $\Delta x_n(0) = 4.0 + 0.1$, $\Delta x_n(1) = 4.0 + 0.1$ for $n = 51$, and the other parameters are specified as: $h_c = 4.0$, $v_{\max} = 2.0$, $\tau = 0.5$.

First, we test the impact of effect coefficient λ of HVT on stability of traffic system while τ_1 is fixed. Fig. 3 displays the patterns of traffic after $t = 10^4$s. Fig. 3(a)–(d) show space–time evolution of velocity in the cases of $\lambda = 0, 0.2, 0.4, 0.6$ and $\tau_1 = 0.5$ respectively. In Fig. 3(a) and (b), when perturbation is added to the traffic system, the stop-and-go traffic wave occurs as time progresses. It is obvious that the width of the stop-and-go wave in Fig. 3(a) is wider than the one in Fig. 3(b), and the amplitude variation trend of density wave is the same as the width. This is so, because the effect of HVT is not considered in Fig. 3(a). In Fig. 3(b) the HVT is introduced, leading to the width of the stop-and-go wave to get smaller, but the fluctuation range remain large. This is due to the effect of HVT not being fully considered. As the effect coefficient λ continues to increase, the amplitude of density wave is greatly weakened. In Fig. 3(d), the phenomenon of stop-and-go traffic disappears completely, and the unstable flow returns to a steady state. Based on the above analysis, we can conclude that traffic stability can increase by taking the effect coefficient of HVT into account.

Following, we study the impact of anticipative time τ_1 on the traffic flow while λ remains unchanged. Fig. 4 shows the velocity evolution after $t = 10^4$ s under different parameters τ_1. Fig. 4(a)–(d) show space–time evolution of velocity corresponding to cases of $\tau_1 = 0, 0.3, 0.6, 0.9$ and $\lambda = 0.3$, respectively. In Fig. 4(a) and (b), we can see that a small perturbation will gradually escalade over time and the uniformly steady-state flow will eventually evolve into stop-and-go waves. The most serious traffic jam occurs in Fig. 4(a). With the help of the forecasting ability, traffic congestion is gradually dissipating (see Fig. 4(b)–(d)), which indicates that the anticipative time plays a positive role in stabilizing the traffic system. In Fig. 4(d), the disturbance disappears eventually, further demonstrating that the anticipative time can enhance traffic stability. These conclusions are all in accordance with the results of the theoretical analysis.

Figs. 3(a) and 4(a) as $\lambda = 0, \tau_1 = 0$, show the case without the impact of HVT, that is the new model reduced to Newell's model. In Figs. 3(b)–(d) and 4(b)–(d), we can see that the intensity of density waves weakens as the parameters λ and τ_1 increase, by considering impact of HVT.

To further study the stabilization impact of the anticipative time and the effect coefficient of HVT on traffic flow, we test the effect of the combination of τ_1 and λ on the traffic system. Setting the values of τ_1 and λ as (0.6, 0.4), (0.5,0.7), the corresponding velocity evolution plot is displayed in Fig. 5. Comparing Figs. 5(a) to 3(b) and 4(b), traffic congestion is found to be relieved significantly in Fig. 5(a). Comparing Figs. 5(b) to 3(c) and 4(c), the traffic congestion disappears completely in Fig. 5(b), indicating that the stabilization of traffic flow can be higher by increasing the anticipative time and the effect coefficient of HVT. This further confirms the positive impact of HVT on stability of traffic flow. These simulation results are also consistent with the theoretical analysis.

Figs. 3 and 4 show that the increase in value of the parameters τ_1, λ can enhance the traffic stability, however, when λ or τ_1 are very low (Figs. 3(b), 4(b)), traffic jam caused by even a slight perturbation still cannot be completely eliminated. This happens because, while λ and τ_1 are low, the regulation of traffic flow is slightly influenced by them, so they cannot convert unstable traffic to uniform traffic. Fig. 6 well demonstrated the abovementioned phenomena. There, it can also be seen that there is a critical curve plotted according to Eq. (14). Once (λ, τ_1) become higher than this critical value, traffic system enters a stable state irrelevant to the size of the added disturbances, while when the values of (λ, τ_1) are lower than the critical value, any size of added disturbances develops into a congestion traffic state.

6. Conclusions

Advanced Connected Vehicle Technology offers new opportunity to improve traffic flow performance. Using the options of the new technology, drivers can get more traffic information from other vehicles than before. Although the anticipate

effect has been researched by scholars, the direct space headway in the future is not considered. By introducing the effect of HVT, this paper proposes a new car-following model to test the impact of HVT on vehicular stream dynamics. The proposed model can predict the driving behavior of the directly leading vehicle, and initiate possible operations in advance. Specifically, the linear stability conditions of the proposed model are obtained, indicating that traffic stability is related to the HVT. Besides the linear analysis, the coexisting critical line is derived by a nonlinear analysis. The results of the analytical method demonstrate that the anticipate interval and the effect coefficient of HVT can both smooth the disturbed traffic system. According to the numerical simulations, we can conclude that, with the help of the HVT effect, the new model can predict the downstream traffic condition so that a driver could avoid an unsuitable reaction to the motion of the leading vehicle. The numerical tests also demonstrate that the extent of traffic congestion is closely related to the power of HVT, which is also well described in the theoretical analysis result.

Before the fully advent of Connected Vehicle Technology, the mixed traffic stream of regular and connected vehicles will coexist for a long time. Therefore, the penetration rate of connected vehicle should be investigated to explore the influence of connected vehicles on mixed traffic stream. Also, the proposed model is not calibrated by field data for these data are difficult to obtain. In the next work, we will try to address this by simulation methods.

Acknowledgment

This research is supported by the National Natural Science Foundation of China (Grant Nos. 71571109, 71871130).

References

[1] T. Nagatani, Modified KdV equation for jamming transition in the continuum models of traffic, Physica A 261 (1998) 599–607.
[2] R. Jiang, Q.S. Wu, Z.J. Zhu, A new continuum model for traffic flow and numerical tests, Transp. Res. B 36 (2002) 405–419.
[3] C.F. Tang, R. Jiang, Q.S. Wu, B. Wiwatanapataphee, Y.H. Wu, Mixed traffic flow in anisotropic continuum model, Transp. Res. Rec. 1999 (2007) 13–22.
[4] T.Q. Tang, H.J. Huang, H.Y. Shang, An extended macro traffic flow model accounting for the driver's bounded rationality and numerical tests, Physica A 468 (2017) 322–333.
[5] T.Q. Tang, L. Caccetta, Y.H. Wu, H.J. Huang, X.B. Yang, A macro model for traffic flow on road networks with varying road conditions, J. Adv. Transp. 48 (2014) 304–317.
[6] T. Nagatani, TDGL and MKdV equation for jamming transition in the lattice models of traffic, Physica A 264 (1999) 581–592.
[7] T. Nagatani, Jamming transition in the lattice models of traffic, Phys. Rev. E 59 (1999) 4857–4864.
[8] J. Zhou, Z.K. Shi, A new lattice hydrodynamic model for bidirectional pedestrian flow with the consideration of pedestrian's anticipation effect, Nonlinear Dynam. 81 (2015) 1247–1262.
[9] D.H. Sun, M. Zhang, T. Chuan, Multiple optimal current difference effect in the lattice traffic flow model, Modern Phys. Lett. B 28 (2014) 1450091.
[10] G.H. Peng, X.H. Cai, B.F. Cao, C.Q. Liu, A new lattice model of traffic flow with the consideration of the traffic interruption probability, Physica A 391 (2012) 656–663.
[11] T. Wang, Z.Y. Gao, W.Y. Zhang, J. Zhang, S.B. Li, Phase transitions in the two-lane density difference lattice hydrodynamic model of traffic flow, Nonlinear Dynam. 77 (2014) 635–642.
[12] H.H. Tian, H.D. Hu, Y.F. Wei, Y. Xue, W.Z. Lu, Lattice hydrodynamic model with bidirectional pedestrian flow, Physica A 388 (2009) 2895–2902.
[13] T. Wang, J. Zhang, Z.Y. Gao, W.Y. Zhang, S.B. Li, Congested traffic patterns of two-lane lattice hydrodynamic model with on-ramp, Nonlinear Dynam. 88 (2017) 1345–1359.
[14] M. Treiber, A. Hennecke, D. Helbing, Derivation, properties, and simulation of a gas-kinetic-based nonlocal traffic model, Phys. Rev. E 59 (1999) 239.
[15] K. Nagel, M. Schreckenberg, A cellular automaton models of traffic flow along a highway containing a junction, Physica A 29 (1996) 3119–3127.
[16] J.F. Tian, R. Jiang, B. Jia, Z.Y. Gao, S.F. Ma, Empirical analysis and simulation of the concave growth pattern of traffic oscillations, Transp. Res. B 93 (2016) 338–354.
[17] J.F. Tian, G.Y. Li, M. Treiber, R. Jiang, N. Jia, S. Ma, Cellular automaton model simulating spatiotemporal patterns, phase transitions and concave growth pattern of oscillations in traffic flow, Transp. Res. B 93 (2016) 560–575.
[18] J.F. Tian, B. Jia, S. Ma, C. Zhu, R. Jiang, Y. Ding, Cellular automaton model with dynamical 2D speed-gap relation, Transp. Sci. 51 (2016) 807–822.
[19] J.F. Tian, N. Jia, N. Zhu, B. Jia, Z.Z. Yuan, Brake light cellular automaton model with advanced randomization for traffic breakdown, Transp. Res. C 44 (2014) 282–298.
[20] A. Reuschel, Fahrzeugbewegungen in der KolonneBeigleichformig beschleunigtem oder vertzogerten, Oesterr. Ing. Archit. 4 (1950) 193–215.
[21] G.F. Newell, Nonlinear effects in the dynamics of car following, Oper. Res. 9 (1961) 145–291.
[22] M. Bando, K. Hasebe, A. Nakayama, A. Shibata, Y. Sugiyama, Dynamical model of traffic congestion and numerical simulation, Phys. Rev. E 51 (1995) 1035.
[23] X.P. Li, Y.F. Ouyang, Measurement and estimation of traffic oscillation properties, Transp. Res. B 44 (2010) 1–14.
[24] X.P. Li, J.X. Cui, S. An, M. Parsafard, Stop-and-go traffic analysis: Theoretical properties, environmental impacts and oscillation mitigation, Transp. Res. B 70 (2014) 319–339.
[25] R. Jiang, M.B. Hu, H.M. Zhang, Z.Y. Gao, B. Jia, Q.S. Wu, On some experimental features of car-following behavior and how to model them, Transp. Res. B 80 (2015) 338–354.
[26] J.F. Tian, M. Treiber, S. Ma, B. Jia, W. Zhang, Microscopic driving theory with oscillatory congested states: model and empirical verification, Transp. Res. B 71 (2015) 138–157.
[27] D.F. Xie, X.M. Zhao, Z.B. He, Heterogeneous traffic mixing regular and connected vehicles: modeling and stabilization, IEEE Trans. Intell. Transp. Syst. (2018) 1–12, http://dx.doi.org/10.1109/TITS.2018.2857465.
[28] R. Jiang, C.J. Jin, H.M. Zhang, Y.X. Huang, J.F. Tian, W. Wang, M.B. Hu, H. Wang, B. Jia, Experimental and empirical investigations of traffic flow instability, Transp. Res. C 94 (2018) 83–98.
[29] R. Li, J.J. Wu, H. Liu, Z.Y. Gao, H.J. Sun, R. Ding, T.Q. Tang, Crowded urban traffic: co-evolution among land development, population, roads and vehicle ownership, Nonlinear Dynam. (2019) 1–13, http://dx.doi.org/10.1007/s11071-018-4722-z.

[30] H.D. Yin, J.J. Wu, H.J. Sun, Y.C. Qu, X. Yang, B. Wang, Optimal bus-bridging service under a metro station disruption, J. Adv. Transp. http://dx.doi.org/10.1155/2018/2758652.
[31] S.P. Yang, J.J. Wu, X. Yang, H.J. Sun, Z.Y. Gao, Energy-efficient timetable and speed profile optimization with multi-phase speed limits: theoretical analysis and application, Appl. Math. Model. 56 (2018) 32–50.
[32] T.Q. Tang, Y.X. Rui, J. Zhang, T. Wang, Impacts of group behavior on bicycle flow at a signalized intersection, Physica A 512 (2018) 1205–1215.
[33] T.Q. Tang, T. Wang, L. Chen, H.J. Huang, Analysis of the equilibrium trip cost accounting for the fuel cost in a single-lane traffic system without late arrival, Physica A 490 (2018) 451–457.
[34] T.Q. Tang, Z.Y. Yi, J. Zhang, T. Wang, J.Q. Leng, A speed guidance strategy for multiple signalized intersections based on car-following model, Physica A 496 (2018) 399–409.
[35] H.X. Ge, S.Q. Dai, Y. Xue, L.Y. Dong, Stabilization analysis and modified Korteweg–de Vries equation in a cooperative driving system, Phys. Rev. E 71 (2005) 066119.
[36] D. Helbing, B. Tilch, Generalized force model of traffic dynamics, Phys. Rev. E 58 (1998) 133–138.
[37] R. Jiang, Q.S. Wu, Z.J. Zhu, Full velocity difference model for a car-following theory, Phys. Rev. E 64 (2001) 017101.
[38] T. Wang, Z.Y. Gao, X.M. Zhao, Multiple velocity difference model and its stability analysis, Acta Phys. Sin. 55 (2006) 0634–07.
[39] X.M. Zhao, Z.Y. Gao, A new car-following model: full velocity and acceleration difference model, Eur. Phys. J. B 47 (2005) 145–150.
[40] P. Redhu, V. Siwach, An extended lattice model accounting for traffic jerk, Physica A 492 (2018) 1473–1480.
[41] T.Q. Tang, C.Y. Li, H.J. Huang, A new car-following model with the consideration of the driver's forecast effect, Phys. Lett. A 374 (2010) 3951–3956.
[42] T.Q. Tang, H.J. Huang, H.Y. Shang, A new macro model for traffic flow with the consideration of the driver's forecast effect, Phys. Lett. A 374 (2010) 1668–1672.
[43] D.H. Sun, C. Tian, A traffic flow lattice model with the consideration of driver anticipation effect and its numerical simulation, Acta. Phys. Sin. 60 (2011) 068901.
[44] L.J. Zheng, C. Tian, D.H. Sun, W.N. Liu, A new car-following model with consideration of anticipation driving behavior, Nonlinear Dynam. 70 (2012) 1205–1211.
[45] G.H. Peng, R.J. Cheng, A new car-following model with the consideration of anticipation optimal velocity, Physica A 392 (2013) 3563–3569.
[46] G.H. Peng, W. Song, Y.J. Peng, S.H. Wang, A novel macro model of traffic flow with the consideration of anticipation optimal velocity, Physica A 398 (2014) 76–82.